NONLINEAR OSCILLATIONS AND ENERGY LOCALIZATION IN CARBON NANOTUBES

Angelo Oreste Andrisano
Department of Engineering "Enzo Ferrari", University of Modena and Reggio Emilia, Italy
E-mail: angelooreste.andrisano@unimore.it

Leonid I. Manevitch
N.N. Semenov Institute of Chemical Physics, Russian Academy of Sciences, Moscow, Russia
E-mail: lmanev@chph.ras.ru

Francesco Pellicano
Department of Engineering "Enzo Ferrari", University of Modena and Reggio Emilia, Italy
E-mail: francesco.pellicano@unimore.it

Matteo Strozzi
Department of Engineering "Enzo Ferrari", University of Modena and Reggio Emilia, Italy
E-mail: matteo.strozzi@unimore.it

Abstract. *In this paper, the low-frequency nonlinear oscillations and energy localizations of Single-Walled Carbon Nanotubes (SWNTs) are analysed. The SWNTs dynamics is studied within the framework of the Sanders-Koiter thin shell theory. The circumferential flexure vibration modes (CFMs) are considered. Simply supported boundary conditions are investigated. Two different approaches are compared, based on numerical and analytical models. The numerical model uses a double series expansion for the displacement fields based on the Chebyshev polynomials and harmonic functions. The Lagrange equations are considered to obtain a set of nonlinear ordinary differential equations of motion which are solved using the implicit Runge-Kutta numerical method. The analytical model considers a reduced form of the shell theory assuming small circumferential and tangential shear deformations. The Galerkin procedure is used to get the nonlinear ordinary differential equations of motion which are solved using the multiple scales analytical method. The natural frequencies obtained by considering the two approaches are compared in linear field. The effect of the aspect ratio on the analytic and numerical values of the localization threshold is investigated in nonlinear field.*

Keywords*: nonlinear oscillations, energy localization, carbon nanotubes*

1. INTRODUCTION

The spatially localized excitations represent one of the most interesting phenomena in the nonlinear dynamics of solids and structures [1]; in particular, the spatial confinement of the

nonlinear vibrations generated by external loads can be used to develop robust shock and vibration isolation designs for certain classes of engineering systems [2].

In the cases of discrete structures, the nonlinear energy localization can be studied in the framework of nonlinear normal modes (NNMs) or limiting phase trajectories (LPTs).

NNMs are usually employed to describe nonlinear elementary stationary processes with a weak energy exchange between coupled oscillators or oscillatory chains, where localized NNMs denote stationary energy localizations [3].

Conversely, LPTs allow to describe nonlinear elementary strongly non-stationary processes with a strong energy exchange between the different parts of finite nonlinear systems, where localized LPTs denote non-stationary energy localizations [4].

The concepts of effective particles and limiting phase trajectories have been extended also to the SWNTs, which represent finite discrete carbon structures consisting of needle-like tubes, described as helical microtubules of graphitic carbon.

Notwithstanding their small size and discrete nature, SWNTs were found to behave similarly to thin walled continuous structures presenting both membrane and bending stiffness; in particular, the analogies between the elastic thin shell model and the SWNT structure led to an extensive application of the continuous shell theories for the SWNTs structural analysis [5].

The effect of the boundary conditions on the nonlinear vibrations of circular cylindrical shells has been deeply investigated in the pertinent literature in the past years; in particular, shells with simply supported (periodic), clamped and free edges have been considered [6].

In the present paper, the low-frequency vibrations and energy localization of SWNTs are investigated on the basis of the Sanders-Koiter shell theory. The CFMs are examined. Simply supported boundary conditions are applied.

Two different approaches are compared. The numerical model uses a double mixed series expansion for the displacement fields based on the Chebyshev polynomials and the harmonic functions. The Lagrange equations are considered to obtain a set of nonlinear ordinary differential equations of motion which is solved by using the implicit Runge-Kutta numerical methods.

The analytical model considers a reduced form of the shell theory assuming small circumferential and tangential shear deformations. The Galerkin procedure is used to obtain the nonlinear ordinary differential equations of motion, which are solved by using the multiple scales analytical method.

The natural frequencies obtained by considering the analytical and numerical approaches are compared.

The effect of the aspect ratio on the analytical and numerical values of the localization threshold are investigated in nonlinear field.

2. SANDERS-KOITER SHELL THEORY

In Figure 1, a circular cylindrical shell having radius R, length L and thickness h is shown; a cylindrical coordinate system (O; x, θ, z) is considered where the origin O of the reference system is located at the centre of one end of the shell.

In Figure 1, three displacement fields are represented: longitudinal u (x, θ, t), circumferential v (x, θ, t) and radial w (x, θ, t), where (x, θ) are the longitudinal and angular coordinates, z is the radial coordinate along the thickness h and t is the time.

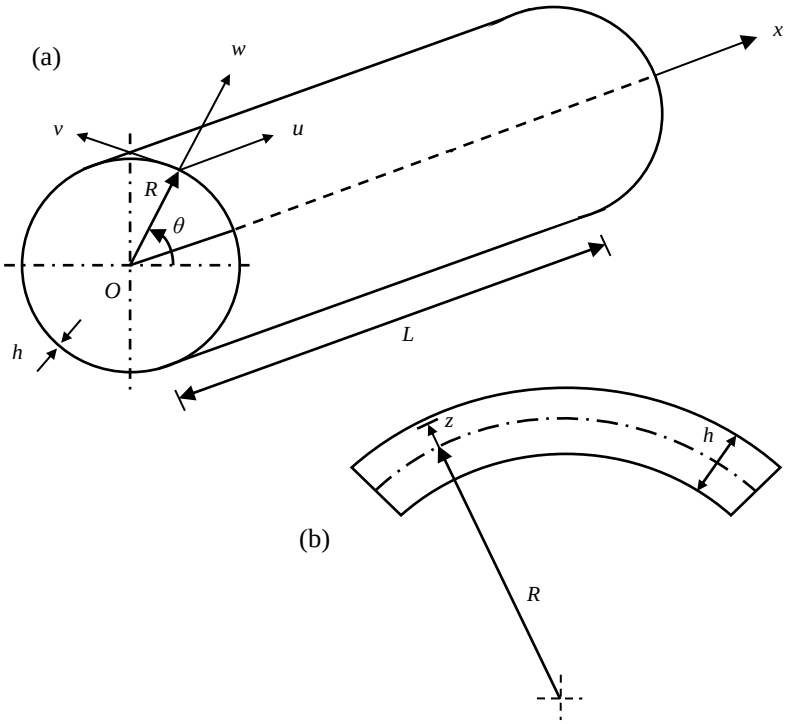

Figure 1. Geometry of the shell. (a) Complete shell; (b) cross-section of the shell surface.

Elastic Strain Energy

The nondimensional elastic strain energy of a cylindrical shell is written in the form

$$\tilde{E} = \frac{1}{2}\frac{1}{(1-\nu^2)}\left[\int_0^1\int_0^{2\pi}\left(\tilde{\varepsilon}_{x,0}^2 + \tilde{\varepsilon}_{\theta,0}^2 + 2\nu\tilde{\varepsilon}_{x,0}\tilde{\varepsilon}_{\theta,0} + \frac{(1-\nu)}{2}\tilde{\gamma}_{x\theta,0}^2\right)d\eta d\theta + \frac{\beta^2}{12}\int_0^1\int_0^{2\pi}\left(\tilde{k}_x^2 + \tilde{k}_\theta^2 + 2\nu\tilde{k}_x\tilde{k}_\theta + \frac{(1-\nu)}{2}\tilde{k}_{x\theta}^2\right)d\eta d\theta\right] \tag{1}$$

where ($\tilde{\varepsilon}_{x,0}$, $\tilde{\varepsilon}_{\theta,0}$, $\tilde{\gamma}_{x\theta,0}$) are the nondimensional middle surface strains, ($\tilde{k}_x$, $\tilde{k}_\theta$, $\tilde{k}_{x\theta}$) are the nondimensional middle surface changes in curvature and torsion and $\beta = h/R$.

Kinetic Energy

The nondimensional kinetic energy of a cylindrical shell is given by

$$\tilde{T} = \frac{1}{2}\gamma\int_0^1\int_0^{2\pi}(\tilde{u}^{'2} + \tilde{v}^{'2} + \tilde{w}^{'2})d\eta d\theta \tag{2}$$

where ($\tilde{u}^{'}, \tilde{v}^{'}, \tilde{w}^{'}$) denote the nondimensional velocity fields and $\gamma = \rho R^2 \omega_0^2 / E$.

Numerical Solution of the Sanders-Koiter Shell Theory

In order to carry out the numerical analysis of the CNT dynamics, a two-steps procedure is applied: i) the three displacement fields are expanded by using a double mixed series, then the Rayleigh-Ritz method is applied in order to obtain an approximation of the linear eigenfunctions; ii) the displacement fields are re-expanded by using the linear approximated eigenfunctions and the Lagrange equations are considered to obtain a set of nonlinear ordinary differential equations of motion.

Linear Vibration Analysis. A modal vibration can be written in the form

$$\tilde{u}(\eta,\theta,\tau) = \tilde{U}(\eta,\theta)\,\tilde{f}(\tau) \qquad \tilde{v}(\eta,\theta,\tau) = \tilde{V}(\eta,\theta)\,\tilde{f}(\tau) \qquad \tilde{w}(\eta,\theta,\tau) = \tilde{W}(\eta,\theta)\,\tilde{f}(\tau) \tag{3}$$

where $\tilde{U}(\eta,\theta)$, $\tilde{V}(\eta,\theta)$, $\tilde{W}(\eta,\theta)$ represent the mode shape and $\tilde{f}(\tau)$ describes the time law.

The mode shape $(\tilde{U}, \tilde{V}, \tilde{W})$ are expanded by means of the Chebyshev polynomials $T_m^*(\eta)$ in the longitudinal direction and the harmonic functions (cos $n\theta$, sin $n\theta$) along the circumferential direction

$$\begin{aligned}
\tilde{U}(\eta,\theta) &= \sum_{m=0}^{M_u}\sum_{n=0}^{N} \tilde{U}_{m,n} T_m^*(\eta)\cos n\theta \\
\tilde{V}(\eta,\theta) &= \sum_{m=0}^{M_v}\sum_{n=0}^{N} \tilde{V}_{m,n} T_m^*(\eta)\sin n\theta \\
\tilde{W}(\eta,\theta) &= \sum_{m=0}^{M_w}\sum_{n=0}^{N} \tilde{W}_{m,n} T_m^*(\eta)\cos n\theta
\end{aligned} \tag{4}$$

where $(\tilde{U}_{m,n},\ \tilde{V}_{m,n},\ \tilde{W}_{m,n})$ are the generalized coordinates.

Boundary Conditions. Simply supported boundary conditions are given by

$$\tilde{w} = 0 \qquad \tilde{v} = 0 \qquad \tilde{M}_x = 0 \qquad \tilde{N}_x = 0 \qquad \eta = 0,1 \tag{5}$$

where the nondimensional force $\tilde{N}_x$ and moment $\tilde{M}_x$ are given by

$$\tilde{N}_x = \tilde{\varepsilon}_{x,0} + \nu\tilde{\varepsilon}_{\theta,0} \qquad\qquad \tilde{M}_x = \tilde{k}_x + \nu\tilde{k}_\theta \tag{6}$$

The previous conditions (5,6) applied to expansions (4) imply the following equations

$$
\begin{aligned}
&\sum_{m=0}^{M_w} \tilde{W}_{m,n} T_m^*(\eta) = 0 \qquad n \in [0,N] \qquad \theta \in [0,2\pi] \qquad \eta = 0,1 \\
&\sum_{m=0}^{M_v} \tilde{V}_{m,n} T_m^*(\eta) = 0 \qquad n \in [0,N] \qquad \theta \in [0,2\pi] \qquad \eta = 0,1 \\
&\sum_{m=0}^{M_w} \tilde{W}_{m,n} T_{m,\eta\eta}^*(\eta) = 0 \qquad n \in [0,N] \qquad \theta \in [0,2\pi] \qquad \eta = 0,1 \\
&\sum_{m=0}^{M_u} \tilde{U}_{m,n} T_{m,\eta}^*(\eta) = 0 \qquad n \in [0,N] \qquad \theta \in [0,2\pi] \qquad \eta = 0,1
\end{aligned}
\tag{7}
$$

The linear system given by the equations (7) can be solved analytically in terms of the linearly dependent coefficients $(\tilde{U}_{1,n},\ \tilde{U}_{2,n},\ \tilde{V}_{0,n},\ \tilde{V}_{1,n},\ \tilde{W}_{0,n},\ \tilde{W}_{1,n},\ \tilde{W}_{2,n},\ \tilde{W}_{3,n})$.

Rayleigh-Ritz Procedure. The maximum number of variables needed for describing a general vibration mode with *n* nodal diameters is given by ($N_p = M_u + M_v + M_w + 3 - p$), with ($M_u = M_v = M_w$) as maximum degree of the Chebyshev polynomials and *p* as number of equations for the boundary conditions to be respected.

A specific convergence analysis was carried out to select the degree of the Chebyshev polynomials: degree 11 was found suitably accurate, ($M_u = M_v = M_w = 11$).

For a multi-mode analysis including different values of nodal diameters *n*, the number of degrees of freedom is computed by the relation ($N_{max} = N_p \times (N + 1)$), where *N* represents the maximum value of the nodal diameters *n* to be considered.

After imposing the stationarity to the Rayleigh quotient, one obtains the eigenvalue problem

$$
(-\omega^2 \tilde{\mathrm{M}} + \tilde{\mathrm{K}})\tilde{\mathrm{q}} = \tilde{0} \tag{8}
$$

which gives approximate natural frequencies (eigenvalues) and modes (eigenvectors).

The vector function

$$
\tilde{\mathrm{Q}}^{(j)}(\eta,\theta) = \begin{bmatrix} \tilde{U}^{(j)}(\eta,\theta) \\ \tilde{V}^{(j)}(\eta,\theta) \\ \tilde{W}^{(j)}(\eta,\theta) \end{bmatrix} \tag{9}
$$

is the approximation of the *j*-th eigenfunction vector of the original problem.

Nonlinear Vibration Analysis. In the nonlinear analysis, the displacement fields $\tilde{u}(\eta,\theta,\tau)$, $\tilde{v}(\eta,\theta,\tau)$, $\tilde{w}(\eta,\theta,\tau)$ are expanded by using the previous linear mode shapes $\tilde{U}^{(j,n)}(\eta,\theta)$, $\tilde{V}^{(j,n)}(\eta,\theta)$, $\tilde{W}^{(j,n)}(\eta,\theta)$ in the form

$$
\tilde{u}(\eta,\theta,\tau) = \sum_{j=1}^{N_u} \sum_{n=1}^{N} \tilde{U}^{(j,n)}(\eta,\theta)\, \tilde{f}_{u,j,n}(\tau)
$$

$$\tilde{v}(\eta,\theta,\tau)=\sum_{j=1}^{N_v}\sum_{n=1}^{N}\tilde{V}^{(j,n)}(\eta,\theta)\,\tilde{f}_{v,j,n}(\tau)$$
$$\tilde{w}(\eta,\theta,\tau)=\sum_{j=1}^{N_w}\sum_{n=1}^{N}\tilde{W}^{(j,n)}(\eta,\theta)\,\tilde{f}_{w,j,n}(\tau) \tag{10}$$

where the modal coordinates $(\tilde{f}_{u,j,n}(\tau),\ \tilde{f}_{v,j,n}(\tau),\ \tilde{f}_{w,j,n}(\tau))$ are unknown functions.

Lagrange Equations. The nondimensional Lagrange equations of motion in the case of free vibrations can be expressed as

$$\frac{d}{d\tau}\left(\frac{\partial\tilde{T}}{\partial\tilde{q}_i^{'}}\right)+\frac{\partial\tilde{E}}{\partial\tilde{q}_i}=0 \qquad i\in[1,N_{\max}] \tag{11}$$

where $N_{\max}$ depends on the modes used in (10) and $(\tilde{q}_i,\tilde{q}_i^{'})$ are nondimensional lagrangian coordinates.

By using the Lagrange equations (11), a set of nonlinear ordinary differential equations of motion is obtained, which is finally solved by implicit Runge-Kutta numerical methods.

3. REDUCED SANDERS-KOITER SHELL THEORY

For the CFMs (n = 2), the nonlinear expansions of the nondimensional displacement fields are

$$\begin{aligned}\tilde{u}(\eta,\theta,\tau)&=\tilde{U}_0(\eta,\tau)+\tilde{U}(\eta,\tau)\cos(2\theta)\\ \tilde{v}(\eta,\theta,\tau)&=\tilde{V}(\eta,\tau)\sin(2\theta)\\ \tilde{w}(\eta,\theta,\tau)&=\tilde{W}_0(\eta,\tau)+\tilde{W}(\eta,\tau)\cos(2\theta)\end{aligned} \tag{12}$$

where $\tilde{U}_0$ and $\tilde{W}_0$ are the axisymmetric component of longitudinal and radial displacements.

By neglecting the nondimensional middle surface circumferential normal strain

$$\tilde{\varepsilon}_{\theta,0}=\frac{\partial\tilde{v}}{\partial\theta}+\tilde{w}=0 \tag{13}$$

and the nondimensional middle surface tangential shear strain

$$\tilde{\gamma}_{x\theta,0}=\frac{\partial\tilde{u}}{\partial\theta}-\alpha\frac{\partial\tilde{v}}{\partial\eta}=0 \tag{14}$$

the nondimensional longitudinal and circumferential displacement fields can be written as functions of the nondimensional radial displacement field.

The nonlinear equation of motion for the nondimensional radial displacement field is written as

$$\frac{\partial^2\tilde{W}}{\partial\tau^2}+\frac{36\beta^2}{5}\tilde{W}-\frac{\alpha^2\beta^2(3+\nu)}{10}\frac{\partial^2\tilde{W}}{\partial\eta^2}+\frac{\alpha^2}{20}\frac{\partial^4\tilde{W}}{\partial\eta^2\partial\tau^2}+$$
$$\frac{\alpha^4(3+4\beta^2)}{60}\frac{\partial^4\tilde{W}}{\partial\eta^4}+\frac{81}{40}\left[\tilde{W}\left(\frac{\partial\tilde{W}}{\partial\tau}\right)^2+\tilde{W}^2\frac{\partial^2\tilde{W}}{\partial\tau^2}\right]-\frac{9\alpha^2}{40}\times$$
$$\left[\frac{\partial^2\tilde{W}}{\partial\tau^2}\left(\frac{\partial\tilde{W}}{\partial\eta}\right)^2+2\frac{\partial\tilde{W}}{\partial\tau}\frac{\partial\tilde{W}}{\partial\eta}\frac{\partial^2\tilde{W}}{\partial\eta\partial\tau}-\tilde{W}\left(\frac{\partial^2\tilde{W}}{\partial\eta\partial\tau}\right)^2+\left(\frac{\partial\tilde{W}}{\partial\tau}\right)^2\frac{\partial^2\tilde{W}}{\partial\eta^2}+\right.$$
$$\left.W\frac{\partial^2\tilde{W}}{\partial\tau^2}\frac{\partial^2\tilde{W}}{\partial\eta^2}+4\alpha^2\left(\frac{\partial\tilde{W}}{\partial\eta}\right)^2\frac{\partial^2\tilde{W}}{\partial\eta^2}\right]-\frac{\alpha^4}{40}\left[\left(\frac{\partial^2\tilde{W}}{\partial\eta\partial\tau}\right)^2\frac{\partial^2\tilde{W}}{\partial\eta^2}+\right.$$
$$2\frac{\partial\tilde{W}}{\partial\eta}\frac{\partial^3\tilde{W}}{\partial\eta\partial\tau^2}\frac{\partial^2\tilde{W}}{\partial\eta^2}-2\alpha^2\left(\frac{\partial^2\tilde{W}}{\partial\eta^2}\right)^3+2\frac{\partial\tilde{W}}{\partial\eta}\frac{\partial^2\tilde{W}}{\partial\eta\partial\tau}\frac{\partial^3\tilde{W}}{\partial\eta^2\partial\tau}+$$
$$\left.\left(\frac{\partial\tilde{W}}{\partial\eta}\right)^2\frac{\partial^4\tilde{W}}{\partial\eta^2\partial\tau^2}-8\alpha^2\frac{\partial\tilde{W}}{\partial\eta}\frac{\partial^2\tilde{W}}{\partial\eta^2}\frac{\partial^3\tilde{W}}{\partial\eta^3}-\alpha^2\left(\frac{\partial\tilde{W}}{\partial\eta}\right)^2\frac{\partial^4\tilde{W}}{\partial\eta^4}\right]=0 \tag{15}$$

This governing partial differential equation allows to calculate the natural frequencies in linear field as well as to estimate the effect of the nonlinearity at different boundary conditions.

Boundary Conditions

The linearization of equation (15) leads to the following expression

$$\frac{\partial^2\tilde{W}}{\partial\tau^2}+\frac{36}{5}\beta^2\tilde{W}-\frac{(3+\nu)}{10}\alpha^2\beta^2\frac{\partial^2\tilde{W}}{\partial\eta^2}+\frac{1}{20}\alpha^2\frac{\partial^4\tilde{W}}{\partial\eta^2\partial\tau^2}+\frac{1}{60}\alpha^4(3+4\beta^2)\frac{\partial^4\tilde{W}}{\partial\eta^4}=0 \tag{16}$$

Assuming the radial displacement $\tilde{W}(\eta,\tau)=\bar{W}(\eta)\cos(\omega\tau)$, equation (16) becomes

$$\bar{W}(\eta)=c_1\cos(\mu\eta+\delta_1)+c_2\exp(-\gamma\eta+\delta_2)+c_3\exp(\gamma\eta+\delta_3) \tag{17}$$

This equation contains both a harmonic-type solution and an aperiodic exponential-type solution in η; the equation should be completed with the suitable boundary conditions.

Simply Supported Edges. Simply supported boundary conditions can be expressed in the terms of the radial displacement $\bar{W}$ as

$$\bar{W}(\eta)=0 \qquad \frac{\partial^2\bar{W}(\eta)}{\partial\eta^2}=0 \qquad \eta=(0,1) \tag{18}$$

Substituting these expressions into equation of motion (17), we get two transcendent equations with respect to parameters μ and γ; these equations are then solved analytically by applying the asymptotic expansion and the multiple scales method, in order to obtain an approximated analytical solution describing the dynamics of low-frequency nonlinear normal modes.

4. NUMERICAL RESULTS

In the first part of this section, the natural frequencies of the simply supported SWNTs obtained considering the analytical and numerical methods are compared; then, the analytical and numerical values of the localization thresholds are compared in nonlinear field for different aspect ratios.

Natural Frequency Spectra

In Figure 2, comparisons between analytical and numerical natural frequencies of SWNT in Ref. [5] with simply supported edges and aspect ratio $L/R = 20$ are reported for CFMs.

From these comparisons, it can be seen that the differences between the analytical and numerical methods are significant only for high values of the longitudinal wave-number (high frequencies), since in these cases the effect of the circumferential and tangential shear deformations is not negligible and therefore the hypotheses of the reduced Sanders-Koiter shell theory cannot be applied.

On the other hand, when the value of the longitudinal wave-number is small (low frequencies), the differences between the two approaches can be neglected.

Therefore, the analytical and numerical approaches show a good correspondence for the low-frequency CFMs in linear field.

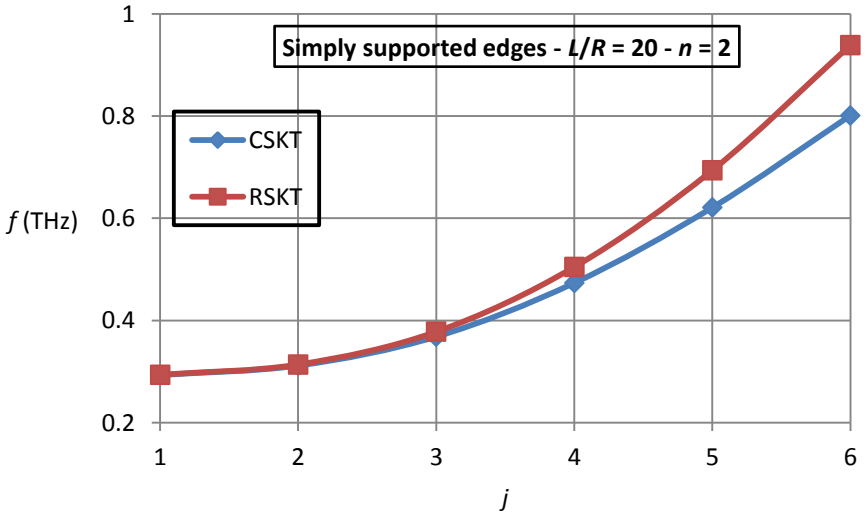

Figure 2. Natural frequencies of the SWNT with simply supported edges of Ref. [5]. Aspect ratio $L/R = 20$. CFMs. "-♦-", complete Sanders-Koiter shell theory (CSKT); "-■-", reduced Sanders-Koiter shell theory (RSKT).

Energy Localization Thresholds

In this part, the analytical and numerical values of the localization thresholds are compared.

These comparisons are carried out in the interval of the aspect ratios $\lambda = 20 \div 110$, where a resonant interaction between the two lowest modes of the frequency spectrum takes place.

In the considered case of simply supported boundary conditions, see Figure 3, a very good correspondence between the results of the analytical and numerical methods can be noted for the interval of the aspect ratios $\lambda = 20 \div 80$, since these boundary conditions are the simplest to be modelled.

Moreover, a fast increase of the value of the localization threshold in the lower region of aspect ratios $\lambda \leq 40$ and an early achievement of the horizontal asymptote $\lambda = 50$ is seen.

Finally, the results of analytical and numerical methods coincide at an aspect ratio $\lambda \geq 80$, since the boundary conditions effect can be neglected far from the edges.

5. CONCLUSIONS

In this paper, the low-frequency oscillations and energy localizations of simply supported SWNTs are analysed in the framework of the Sanders-Koiter elastic thin shell theory. The circumferential flexure modes are studied. Numerical and analytical models are compared.

The natural frequencies obtained by considering the previous methods are different for high longitudinal wave-numbers involving not negligible circumferential and tangential shear deformation effects. Conversely, the two methods show a good correspondence for low longitudinal wave-numbers.

The analytical and numerical values of the localization thresholds coincide at high aspect ratios, since the boundary effects can be neglected far from the edges. Moreover, a very good correspondence between the methods in the intermediate interval, a fast increase of the localization threshold in the lower region and an early achievement of the horizontal asymptote can be seen.

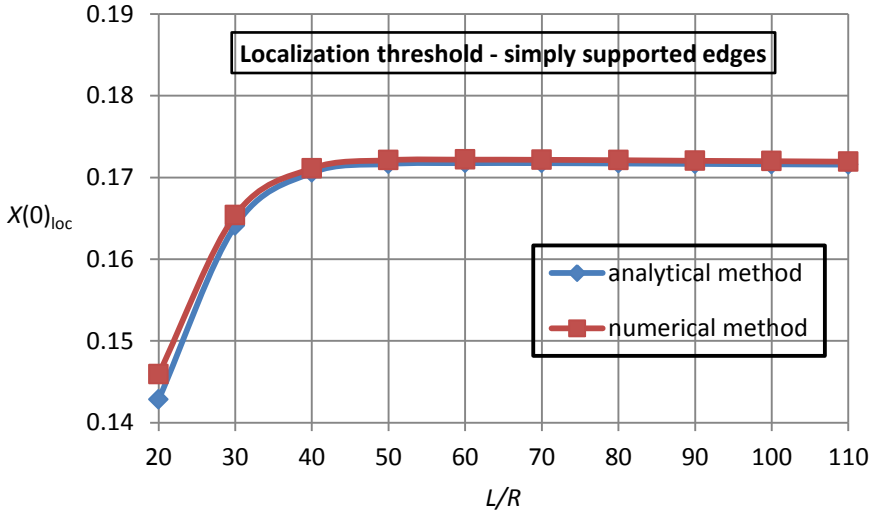

Figure 3. Effect of the aspect ratio on the amplitude of the localization thresholds for the SWNT with simply supported edges of Ref. [5]. "-♦-", analytical results (RSKT); "-■-", numerical results (CSKT).

REFERENCES

[1] Manevitch LI, Gendelman OV, 2011. Tractable Models of Solid Mechanics. Formulation, Analysis and Interpretation.

[2] Balandin DV, Bolotnik NN, and Pilkey WD, 2001. *Optimal Protection From Impact, Shock, and Vibration*.

[3] Jiang D, Pierre C, and Shaw SW, 2005. "Nonlinear normal modes for vibratory systems under harmonic excitation", *Journal of Sound and Vibration*, **288**, pp. 791-812.

[4] Manevitch LI, Smirnov VV, 2010. "Limiting phase trajectories and the origin of energy localization in nonlinear oscillatory chains", *Physical Review E*, **82**, pp. 1-9.

[5] Strozzi M, Manevitch LI, Pellicano F, Smirnov VV, and Shepelev DS, 2014. "Low-frequency linear vibrations of Single-Walled Carbon Nanotubes: analytical and numerical models", *Journal of Sound and Vibration*, **333**, pp. 2936-2957.

[6] Strozzi M, Pellicano F, 2013. "Nonlinear vibrations of functionally graded cylindrical shells", *Thin-Walled Structures*, **67**, pp. 63-77.